Phosphorylation on Carboxyl Terminus Domains of Neurofilament Proteins in Retinal Ganglion Cell Neurons In Vivo: Influences on Regional Neurofilament Accumulation, Interneurofilament Spacing, and Axon Caliber

Ralph A. Nixon,*‡ Peter A. Paskevich, Ram K. Sihag,* and Christina Y. Thayer

Laboratories for Molecular Neuroscience, McLean Hospital, *Department of Psychiatry and ‡Program in Neuroscience, Harvard Medical School, Belmont, Massachusetts 02178

Abstract. The high molecular weight subunits of neurofilaments, NF-H and NF-M, have distinctively long carboxyl-terminal domains that become highly phosphorylated after newly formed neurofilaments enter the axon. We have investigated the functions of this process in normal, unperturbed retinal ganglion cell neurons of mature mice. Using in vivo pulse labeling with [^{35}S]methionine or [^{32}P]orthophosphate and immunocytochemistry with monoclonal antibodies to phosphorylation-dependent neurofilament epitopes, we showed that NF-H and NF-M subunits of transported neurofilaments begin to attain a mature state of phosphorylation within a discrete, very proximal region along optic axons starting 150 μm from the eye. Ultrastructural morphometry of 1,700–2,500 optic axons at each of seven levels proximal or distal to this transition zone demonstrated a threefold expansion of axon caliber at the 150-μm level, which then remained constant distally. The numbers of neurofilaments nearly doubled between the 100- and 150-μm level and further increased a total of threefold by the 1,200-μm level. Microtubule numbers rose only 30–35%. The minimum spacing between neurofilaments also nearly doubled and the average spacing increased from 30 nm to 55 nm. These results show that carboxyl-terminal phosphorylation expands axon caliber by initiating the local accumulation of neurofilaments within axons as well as by increasing the obligatory lateral spacing between neurofilaments. Myelination, which also began at the 150-μm level, may be an important influence on these events because no local neurofilament accumulation or caliber expansion occurred along unmyelinated optic axons. These findings provide evidence that carboxyl-terminal phosphorylation triggers the radial extension of neurofilament sidearms and is a key regulatory influence on neurofilament transport and on the local formation of a stationary but dynamic axonal cytoskeletal network.

THE generation of cells with extreme polar shapes requires highly specialized structural proteins and unique mechanisms for regulating the sorting, assembly, and transport of these proteins. Among the most striking examples of structural specialization are neurofilaments. In most non-neuronal cells, a single subunit composes the intermediate filament network that serves as an intracellular framework and helps to regulate cell shape (Lazarides, 1982; Skalli and Goldman, 1991). In neurons, however, two additional high molecular mass subunits, 140–165 kD (NF-M)[1] and 200–210 kD (NF-H), assemble with the 70-kD core subunit (NF-L) to generate neurofilaments (Hoffman and Lasek, 1975; Liem et al., 1978). Although all three subunits share a central α-helical region and a short variable domain at the amino-terminal end, the two large subunits are distinguished from NF-L and subunits of other intermediate filament classes by the exceptional length of their carboxyl-terminal tail domains (Shaw, 1991; Geisler et al., 1983; Franke, 1987; Steinert and Roop, 1988). These carboxyl-tail domains are localized peripherally along the filament core (Willard and Simon, 1981; Sharpe et al., 1982) and are believed to form radially projecting sidearms that maintain a minimum space between individual neurofilaments (Pant et al., 1978; Leterrier et al., 1982; Liem and Hutchinson, 1982; Sharpe et al., 1982; Julien and Mushynski, 1983; Hirokawa et al., 1984).

Neurofilament behavior is regulated in a complex way by phosphorylation (for reviews see Nixon and Sihag, 1991; Nixon, 1993). Each subunit is phosphorylated, but NF-M

Address all correspondence to Dr. Ralph A. Nixon, Laboratories for Molecular Neuroscience, McLean Hospital, 115 Mill Street, Belmont, MA 02178.

1. *Abbreviations used in this paper*: MPR, multiphosphorylation repeat; NF-H, high molecular mass subunit; NF-L, low molecular mass subunit; NF-M, middle molecular mass subunit.

and NF-H, containing up to 15 and 50 mol of phosphate, respectively, are among the most extensively phosphorylated proteins in the brain (Julien and Mushynski, 1983; Carden et al., 1985). The amino-terminal head domains of NF-L and NF-M contain multiple phosphorylation sites involving protein kinases distinct from those that phosphorylate the carboxyl-terminal domains (Sihag and Nixon, 1989, 1990, 1991). A role has been suggested for amino-terminal head domain phosphorylation in subunit polymerization (Sihag and Nixon, 1989; Gill et al., 1990; Hisanaga et al., 1990; Nakamura et al., 1990). In keeping with their distinctive structure (Geisler et al., 1983; Lees et al, 1988; Mack et al., 1988), the carboxyl-terminal ends are regulated differently and seem to have quite different functions. Many of the phosphate groups on NF-M and NF-H tail domains are added to a series of repeated KSP motifs (Geisler et al., 1987; Lee et al., 1988), which may not all be functionally equivalent (Dahl et al., 1986; Goldstein et al., 1987; Geisler et al., 1987; Lee et al., 1987, 1988; Landmesser and Swain, 1992).

Most phosphate groups are added to NF-M and NF-H tail domains only after neurofilaments have entered the axon (Sternberger and Sternberger, 1983; Lee et al., 1986; Glicksman et al., 1987; Oblinger et al., 1987; Nixon et al., 1987, 1990), and these phosphates are subsequently turned over slowly relative to those at the amino-terminal end (Nixon and Lewis, 1986; Sihag and Nixon, 1991). In mouse retinal ganglion cells, continued phosphorylation of the tail domains during neurofilament transport generates at least four different phosphorylated variants each of NF-H and NF-M (Nixon et al., 1982; Lewis and Nixon, 1988). The most phosphorylated variants are associated with neurofilaments that leave the transport carrier and reside in axons for months, while neurofilaments containing less phosphorylated variants principally move at rates typical of slow axonal transport and reside more briefly in axons (Lewis and Nixon, 1988). These findings suggested that carboxyl-terminal phosphorylation regulates the relative strength of neurofilament interactions with the transport carrier and with stationary axonal structures and thereby controls the rate of movement and residence time of neurofilaments within axons (Lewis and Nixon, 1988; Nixon and Sihag, 1991).

Neurofilaments are well suited for filling space, a particularly valued function in long axons where axoplasmic volume may be orders of magnitude larger than perikaryal volume. The exponential increase in axoplasmic volume as axon caliber expands during development enormously increases the demand for structural elements. Neurons respond by upregulating neurofilament mRNA and protein synthesis (Lasek et al., 1983; Julien et al., 1986; Lieberburg et al., 1989; Schlaepfer and Bruce, 1990), and slowing the rate of neurofilament transport (Willard and Simon, 1983; Hoffman et al., 1984, 1985*a*). Changing filament number alone, however, may not be sufficient to regulate axon caliber completely. For example, overexpressing the NF-L gene in transgenic mice markedly increases NF-L–containing filaments but minimally alters axon caliber (Monteiro et al., 1990). The high molecular weight subunits and especially NF-H seem critically important. The burst of radial axon growth during development and a slower rate of axonal transport (Willard and Simon, 1983; Hoffman et al., 1984, 1985*a*) coincide with the increased expression of NF-H (Shaw and Weber, 1982; Willard and Simon, 1983). Phosphorylation of NF-H and NF-M occurs even later in development (Carden et al., 1985; Dahl and Bignami, 1986; Dahl et al., 1986; Foster et al., 1987) and has been proposed as an additional determinant of axon caliber (Sternberger and Sternberger, 1983; Hoffman et al., 1985*a*; Carden et al., 1985, 1987; deWaegh et al., 1992).

To investigate the function of carboxyl-terminal domain phosphorylation, we took advantage of the anatomy of the visual system, where a homogeneous population of axons from a single class of neurons, the retinal ganglion cells, converge to form the optic nerve. Although the most proximal part of the ganglion cell axon is intraretinal, we found that carboxyl-terminal phosphorylation is sufficiently delayed that the region of the axon where these events occur for most ganglion cells is located in the proximal optic nerve. A relatively sharp transition from immature to mature states of NF-H phosphorylation in this region isolated carboxyl-terminal phosphorylation events from phosphorylation events affecting other regions of neurofilament subunits (Nixon and Sihag, 1991). This enabled us to determine how carboxyl-terminal phosphorylation may regulate neurofilament structure and function in mammalian central neurons under normal, unperturbed conditions in vivo. Portions of this study have appeared earlier in abstract form (Nixon, R. A., P. Paskevich, R. K. Sihag, and T. Wheelock. 1991. Morphologic correlates of neurofilament carboxyl terminal phosphorylation. *J. Cell Biol.* 115:356a).

Materials and Methods

Intravitreal Isotope Injection/Pulse Radiolabeling

Radiolabeled amino acids were injected intravitreally into anesthetized male and female C57Bl/6J mice, aged 10–14 wk, with a glass micropipette apparatus (Nixon, 1980). Mice received 0.25 μl of phosphate-buffered normal saline (pH 7.4) which contained 50–100 μCi of L-[^{35}S]methionine (specific activity 400 Ci/mmol), or 50 μCi of [^{32}P]orthophosphate (specific activity 1,000 Ci/mmol) purchased from New England Nuclear (Boston, MA).

Tissue Preparation

Mouse breeding, maintenance, and dissections of retina and optic axons have been previously described (Nixon, 1980; Nixon and Logvinenko, 1986). Cytoskeletal proteins and Triton-soluble protein fractions were prepared from retinas and optic axons by the method of Chiu and Norton (1982). To minimize proteolysis, buffers in all experiments contained 50 μg/ml leupeptin, 0.5 mM PMSF and 2.5 μg/ml aprotinin.

Polyacrylamide Gel Electrophoresis and Radioactivity Measurements

One-dimensional SDS-PAGE was performed by the procedure of Laemmli (1970) using 320-mm slab gels containing 5–15% or 3–7% polyacrylamide gradients as previously described (Nixon et al., 1982). Proteins labeled with [^{35}S]methionine were detected by autoradiography. In some experiments, relative radioactivity of proteins was calculated from autoradiograms by densitometry as previously described (Nixon et al., 1990).

Immunoprecipitation and Immunoblot Analysis

Neurofilament proteins were immunoprecipitated as previously described (Nixon et al., 1990) using an antiserum raised against chicken antigen which recognized all three NFP subunits (Dahl et al., 1984), and an antiserum raised against bovine NF-H, which primarily recognized NF-H (Dahl, 1981). Immunoblot analyses were performed as described by Takeuchi et al. (1992).

Immunocytochemistry

Mice were anesthetized with halothane gas, the thoracic cavity was exposed, and intracardially injected with 0.5 ml of 2% sodium nitrate (vasodilator) with 50 U of heparin (Upjohn). Mice were perfused intracardially with 60 ml of 10% formalin at room temperature. The retina and optic nerve were dissected out to the level of the optic chiasm and the resultant segment was cryoprotected in 30% sucrose in 10% formalin for several days. Sagittal 8-μm sections were cut on an IEC Minotome cryostat and picked up on glass slides. Immunocytochemical studies were performed using monoclonal antibodies directed against phosphorylation-dependent epitopes on the carboxyl terminus of NF-H and NF-M (SMI-31, SMI-32, RT 97) or a polyclonal antisera directed against NF-H. Immunoreactivity was demonstrated using a modification of the avidin-biotin technique of Hsu et al. (1981) and Vectastain kits (Vector Laboratories, Inc., Burlingame, CA) with diaminobenzidine as the chromogen. Negative controls consisted of tissue sections incubated in the absence of primary antisera.

Electron Microscopy

Mice were anesthetized with halothane gas, injected with sodium nitrite/heparin (protocol as above), and perfused intracardially with 4% paraformaldehyde, 5% glutaraldehyde in 0.1 M cacodylate buffer, pH 7.4 at room temperature. The ocular region was then grossly dissected to expose the eye and optic pathway which were then immersed in the same fixative for an additional 5 h. The retina, optic nerve, and optic tract were then dissected out as a unit structure, rinsed through several buffer changes, and fixed after one hour with 1% OsO_4 in 0.1 M cacodylate buffer, pH 7.4, at room temperature. The unit structure was segmented as described above, and the samples were processed through an ascending ethanol dehydration series, cleared with propylene oxide and embedded in Medcast resin (Ted Pella, Inc., Tustin, CA). Sections were cut on a Reichert-Jung Ultracut-E ultra-microtome. Semi-thin sections (0.5 μm) were stained with 1% toluidine blue. Ultra-thin sections (60 nm) were contrasted with lead citrate and uranyl acetate and examined in a JEOL JEM1200EX electron microscope.

Semi-thin and ultra-thin sections from retinal/optic nerve samples processed for electron microscopy as described above were collected at 25-μm intervals beginning 1.2 mm distal to the retina using an ultramicrotome equipped with a digitally displayed advance totalizer. For purposes of standardization, the retinal excavation was chosen as the structural landmark from which all other levels were measured. The excavation level was defined as that first cross-sectional profile of the optic nerve showing this structure surrounded completely by retinal tissue.

Axon Caliber Measurements

To determine axon caliber distribution, 1,700–2,500 axon profiles were quantified for cross-sectional area at each axon level. Axonal fields were selected evenly from all regions of the cross-section, using the mesh gridbars as super-imposed divisional landmarks. Populations of more than 500 randomly selected axons have been shown to accurately represent the total optic axon population (Nixon and Logvinenko, 1986). Ten non-overlapping microscopic fields from each level were photographed at low power and printed at a final magnification of 18,000×. All myelinated and unmyelinated axons from the field were measured unless the angle of transection was clearly oblique (less than 5% of the population). In some experiments myelinated and unmyelinated fibers were analyzed separately. Axonal areas were measured using an IBM-compatible computer with Bioquant (R and M Biometrics) software and a Summagraphics supergrid digitizing tablet peripheral. Histograms were constructed from the resultant data. The percentage of axons in each of a series of equally spaced size categories was determined at the seven levels of each optic pathway. Histograms were constructed by plotting these percentages as a function of axonal caliber.

Neurofilament and Microtubule Quantification

At each axonal level, between 345 and 539 retinal ganglion cell axon profiles were selected for analysis from the larger population of profiles solely on the basis that neurofilaments and microtubules appeared unequivocally in cross-section throughout the axoplasm or if vesicular organelles occupied more than 50% of the area (<5% excluded on this basis). All regions of the optic nerve section were used in obtaining sample profiles and all axons meeting the minimal inclusion criterion were analyzed in each micrograph. Additional axons of a particular caliber were analyzed, in some cases, to generate a sample of axons with the same distribution of calibers as that in the whole fiber population in the optic nerve. Histograms of caliber distribution for these samples similar to the ones constructed above verified this fact for each axonal level. Microtubules and neurofilaments were counted from randomly assorted photomicrographs at 80,000× by a single investigator. Repetitions were accurate to ±2.5%. A total of 57,973 neurofilaments and 57,849 microtubules were counted in 2,439 axon profiles at 6 levels. Additional analyses were carried out on the unmyelinated fiber subpopulation at the 200 μm and 1,200 μm levels.

Nearest Neighbor Analysis

Twenty-five consecutive axon profiles were selected at the six different axonal levels to include sizes representative of the entire caliber range at that level. Additional groups of 25–40 unmyelinated and myelinated fibers were similarly selected for quantification to obtain the results in Table I. In each axon, the distance from every neurofilament to its nearest neurofilament "neighbor" was measured with a Summagraphics Supergrid digitizing tablet using a software program developed for this purpose (Paskevich, P. A., unpublished observations). For each axon, these distance values were sorted

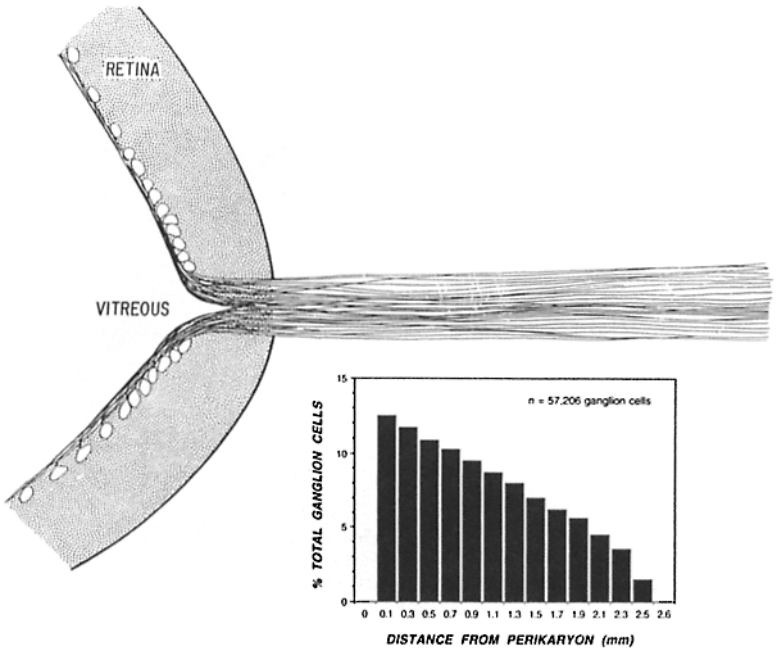

Figure 1. Schematic of the retino-optic junction depicting the relative distribution of ganglion cells and important landmarks. The percentages of retinal ganglion cell bodies at particular distances from the retinal excavation are based on the data of Dräger and Olsen (1981) (modified by permission).

into 5-nm bins, and the percentage of total neurofilaments exhibiting distances falling within each bin was then calculated. In separate calculations, nearest neighbor distances for all neurofilaments in all axons at each level were pooled and the distribution of distances within 5-nm bins was determined. Data are expressed as mean values ± SD.

Results

Anatomic Relationships of Ganglion Cell Fibers at the Retino-Optic Junction

The perikarya of retinal ganglion cells are situated in a concentric gradient of increasing cell density from the periphery of the retina to its center, the optic disk (Dräger and Olsen, 1981) (Fig. 1). The intraretinal portions of ganglion cell axons vary in length from 0.1 to 2.6 mm but more than 55% are less than 0.9 mm (Fig. 1). These axons, converging at the retinal excavation, emerge from the eye to form the optic nerve and optic tract (optic pathway) that extends ~13 mm from the eye to the lateral geniculate nucleus in the adult mouse (Fig. 2). The ganglion cell axons are unmyelinated within the retina and remain so for a distance of ~150–200 μm after they emerge from the eye as the proximal optic nerve (Fig. 2). Between 50 μm and 150 μm, a syncytium of astroglia called the lamina cribrosa ensheathes the axons (Radius, 1981). The appearance of myelin beginning 150 μm from the retinal excavation coincides with an apparent expansion of optic nerve diameter (Fig. 2).

Carboxyl-Terminal Domains of NF-H and NF-M Begin to be Extensively Phosphorylated at a Discrete, Very Proximal Region of Optic Axons

Newly synthesized neurofilament proteins, radiolabeled in vivo by injecting mice intravitreally with [^{35}S]methionine, appeared in the optic nerve in small numbers within 2–6 h (Fig. 3 *B*), presumably from the 15% of ganglion cells situated close to the retinal excavation (Fig. 1). As these radiolabeled subunits moved within the first 1–2 mm of the optic nerve between 1–2 d (Fig. 3 *A*), modifications occurred that resulted in the appearance of mature isoforms of NF-M and NF-H (Fig. 3 *B*). The first newly synthesized NF-M entering optic nerve displayed the same apparent molecular mass (139 kD) as unmodified or dephosphorylated NF-M (Nixon et al., 1990). Major NF-M phosphovariants, identified by their slower electrophoretic mobility, appeared by 8 h after isotope administration and approximated the proportions present in isolated neurofilaments by 12 h (Nixon et al., 1990). The major mature phosphovariants of ^{35}S-labeled NF-H (Lewis and Nixon, 1988) were first detected only after 18–24 h (Fig. 3 *B*).

Neurofilament protein phosphorylation was also monitored in vivo by $^{32}P_i$-labeling after injecting mice intravitreally with [^{33}P]orthophosphate. Neurofilament proteins in the optic nerve were rapidly labeled due to the fact that ATP-containing intermediates are transported at a faster rate than neurofilament proteins and phosphorylate preexisting

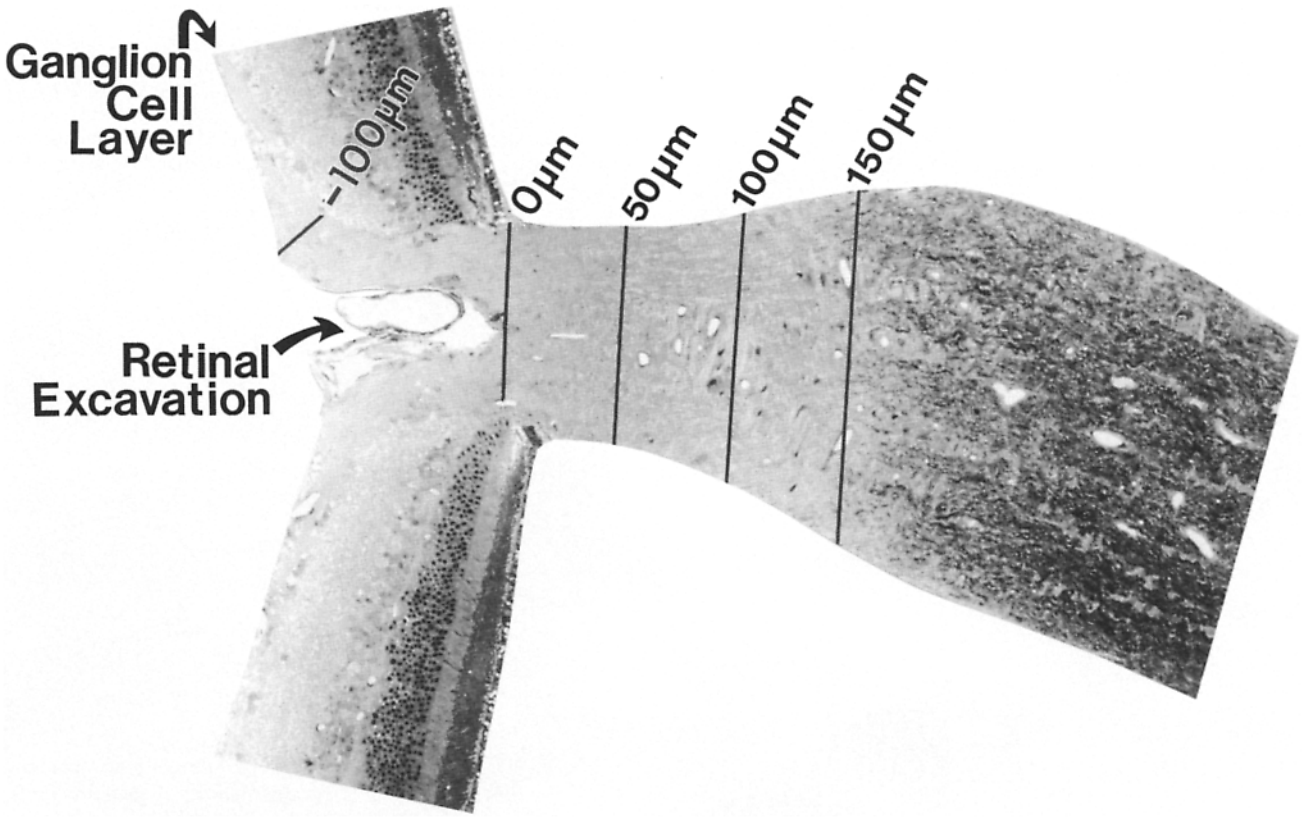

Figure 2. Anatomy of the retino-optic junction in a plastic-embedded 1-μm sagittal section through the eye and optic nerve stained by toluidine blue. Five of the levels analyzed morphometrically in later experiments are shown. Ensheathment of axons by myelin, indicated by dense axonal staining, begins at 150 μm.

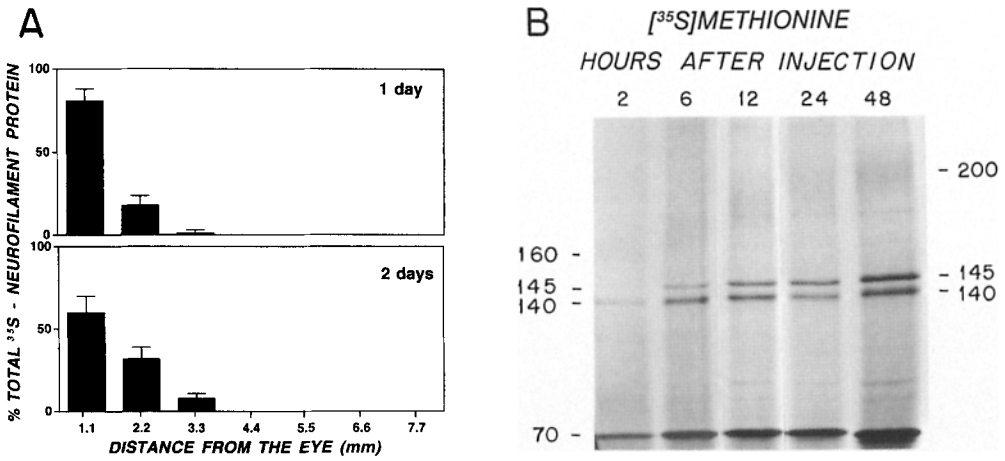

Figure 3. Progressive post-translational modification of [^{35}S]methionine-labeled neurofilament proteins in optic axons at different time intervals after synthesis. *A* shows the proportion of radioactive neurofilament proteins (sum of NF-L, NF-M, and NF-H) in consecutive 1.1-mm segments of the optic nerve 1 or 2 d after intravitreous injection of isotope. After SDS-PAGE and autoradiography, radioactivity in neurofilament proteins was quantitated by densitometry (see Materials and Methods). In *B*, Triton-insoluble fractions of optic nerve were obtained from mice injected intravitreously with [^{35}S]methionine and sacrificed after the indicated time interval. Fractions were immunoprecipitated with a mixture of polyclonal anti-neurofilament antibodies R37 and R96. Labeled proteins were subjected to SDS-PAGE (3–7% polyacrylamide) and autoradiography. Because the efficiency of immunoprecipitation may vary with the phosphorylation state of the proteins, absolute radioactivity of proteins cannot be accurately compared at different time points. The 12-h time point reflects a longer film exposure time than the other time points to facilitate comparison of NF-H mobilities.

axonal neurofilaments (Nixon et al., 1987). At six postinjection time points between 1 and 9 d (two are shown in Fig. 4), the total $^{32}PO_4$ label associated with NF-H subunits, and the ratio of radio-label in NF-H to that in NF-M and NF-L were consistently lower in the most proximal 1-mm optic nerve segment than in more distal segments, particularly beyond 1 day after injection. Lower incorporation into NF-H was not explained by a smaller proportion of NF-H subunits relative to NF-M and NF-L at proximal axonal levels based on previous data (Nixon and Logvinenko, 1986). The most proximal 2 mm of the optic nerve also contained a greater proportion of hypophosphorylated variants of NF-H and NF-M, identified by their more rapid electrophoretic mobility (Kaufman et al., 1984), compared to distal axonal levels (Fig. 4). The ratio of ^{32}P incorporation into the more phosphorylated NF-M variants to the less phosphorylated variants (bracketed in Fig. 4) was between 1 and 2.0 in the first two segments but increased to 3 or more in the subsequent segments at 1 or 2 d after injection. A similar but less pronounced effect on NF-H was seen at day 1.

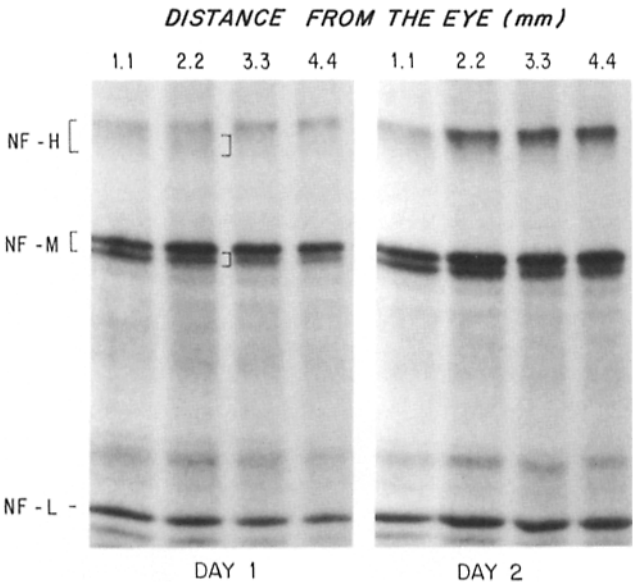

Figure 4. Relative ^{32}P incorporation into neurofilament subunits after injecting mice intravitreously with [^{32}P]orthophosphate. At 1 and 2 d indicated intervals after injection, consecutive 1.1-mm segments of optic nerve were subjected to SDS-PAGE (3–7% polyacrylamide) and autoradiography. Lower molecular weight (hypophosphorylated) isoforms of NF-H and NF-M are more abundant in the first two segments compared to more distal segments, as indicated by brackets on the figure. In the first segment, ^{32}P incorporation is low in NF-H relative to NF-M and NF-L.

To define the region of active phosphorylation more precisely, cryostat sections were cut sagittally from retinas of perfused mice and immunostained using monoclonal antibodies specifically against phosphorylation-dependent epitopes on the carboxyl-terminal domains of NF-H and NF-M (Fig. 5). SMI32 recognizes an NF-H epitope that becomes masked (i.e., immunostaining disappears) when the tail domain is phosphorylated (Sternberger and Sternberger, 1983; Sternberger et al., 1985). In earlier analyses of retinal whole-mounts (Nixon et al., 1990), this antibody decorated ganglion cell perikarya and intraretinal portions of ganglion cell axons. The results in Fig. 5 *A* confirmed these findings and also showed that SMI-32 immunoreactivity in the optic nerve diminished sharply starting ~200 μm downstream from the retinal excavation. A second antibody (RT97) directed against a NF-H epitope that is recognized only when the carboxyl terminal tail is phosphorylated (Anderton et al., 1982; Harris et al., 1991) yielded an immunostaining pattern completely to that of SMI-32 (Fig. 5 *B*). RT97 did not recognize ganglion cell bodies or intraretinal portions of ganglion cell axons and only began to decorate these axons within the optic nerve beginning ~200 μm from the retinal excavation. By comparison, polyclonal antibodies recognizing phosphorylation-dependent and -independent epitopes on NF-M and NF-H (MN 200) and NF-L (not shown) stained the entire length of ganglion cell axons in the retina and optic nerve (Fig. 5 *C*). These data demonstrated a rather

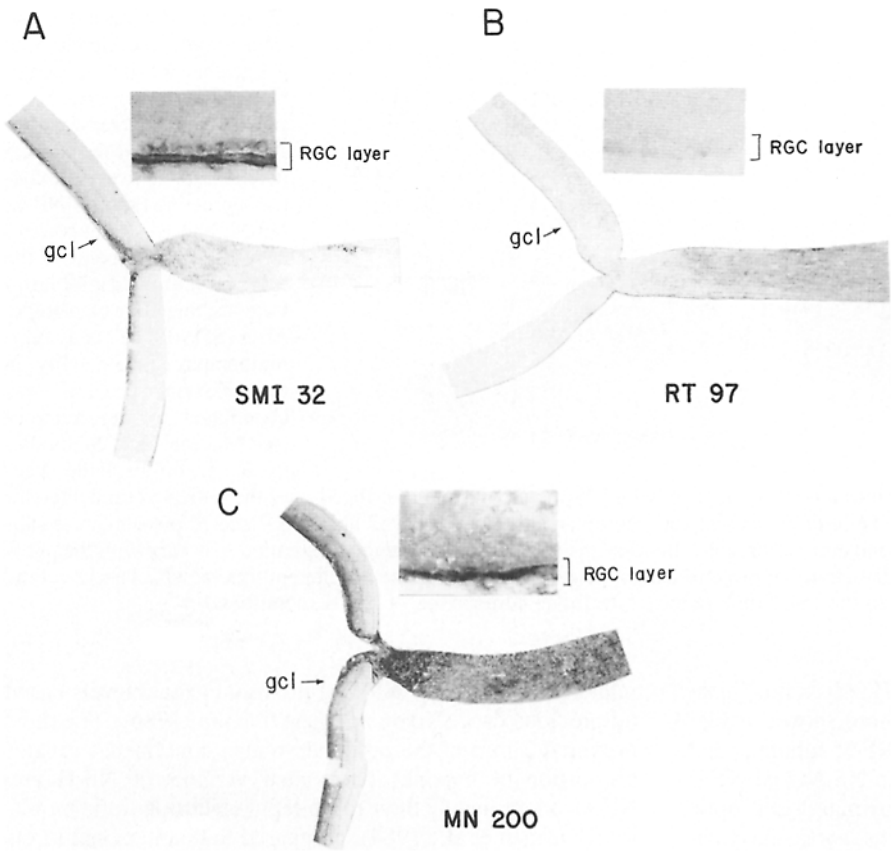

Figure 5. Immunohistochemistry with neurofilament antibodies recognizing different phosphorylation states of NF-H and NF-M. Sagittal 5-μm cryostat sections of the eye and optic nerve were immunostained (see Materials and Methods) by SMI32 (*A*) which recognizes an epitope on the carboxyl-terminal domain that becomes masked by phosphate addition. Immunostaining of retinal ganglion cells and intraretinal portions of their axons is strong (*inset*) but becomes undetectable in the optic nerve beyond a level 150 μm from the retinal excavation. Immunostaining with the monoclonal antibody RT97, which recognizes phosphorylated carboxyl-terminal domains, shows the reverse pattern (*B*). A polyclonal antiserum (*MN 200*) recognizing NF-H independently of its phosphorylation state strongly stains both ganglion cell bodies and axons in their entirety (*C*). Bar, 1 mm = 13.3 μm.

distinct transition zone at the 150–200 μm level proximal to which relatively hypophosphorylated NF-H (and NF-M) isoforms predominated and distal to which neurofilaments were composed of highly phosphorylated variants of these subunits.

Axon Caliber Expands Abruptly and Markedly as NF-H and NF-M Carboxyl-Terminal Domains Achieve Mature States of Phosphorylation

We then compared the organization of the neurofilament network at levels of the optic nerve proximal and distal to this transition zone to investigate the morphological correlates of carboxyl-terminal domain phosphorylation. Six levels along a 1,200-μm length of proximal optic nerve and a more proximal level within the retina were analyzed morphometrically. To determine the distribution of axon caliber sizes, the cross-sectional areas of ~2,500 axons at each of the seven axonal levels were measured. Because the axonal populations studied at every level were very large and representative of the total fiber population in the optic nerve, the comparisons made between the levels accurately reflected the changes taking place along an individual axon.

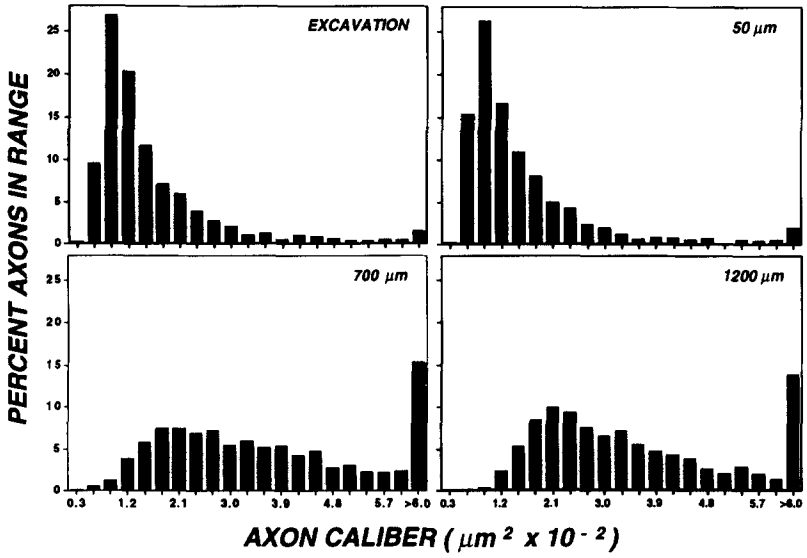

Figure 6. Distribution of axon calibers at four proximal levels along the optic nerve. The number of axons in each size class, expressed as a percentage of total axon population analyzed, is plotted as a function of axon cross-sectional area. From 2,500 to 3,000 axons were analyzed at each level in two animals.

Caliber distributions at different levels of optic nerve were clearly distinguishable (Fig. 6). At each of the three most proximal levels (0, 50, 100 μm), 55% of the axons displayed cross-sectional areas of ≤0.012 μm², while at the three levels between 150 and 1,200 μm only 3% were this small. The mean axon caliber (0.398 μm²) was 2.7-fold larger at the 1,200 μm level than at 50 μm (0.148 μm²). The caliber distribution of fibers at an intraretinal level (−100 μm) resembled that of the proximal optic nerve levels although mean axonal caliber was slightly higher (0.252 μm²). The higher mean caliber may partly reflect an increased abundance of vesicular organelles that were present in axon profiles, many of which were at levels very close to the perikarya. To analyze further how caliber size changed along axons, the data from individual axons were pooled at each level and compared (Fig. 7). These compiled data indicate that axon caliber abruptly expanded ~2.5-fold at 150 μm and remained constant thereafter, even at distal levels within the optic tract (e.g., 7 mm from the eye), which were analyzed in a previous study (Nixon and Logvinenko, 1986).

Marked Neurofilament Accumulation Accompanies Carboxyl-Terminal NF-H Phosphorylation

We counted neurofilaments and microtubules in 308-539 axons at each of the six levels of the proximal optic nerve. The number of neurofilaments rose sharply at the same axonal level (150 μm) where carboxyl-terminal phosphorylation became extensive and axon caliber expanded (Fig. 8). After this sharp increase, neurofilament number rose gradually to a total of threefold by the 1,200 μm level. By contrast, microtubules increased only 30–35% within the same region.

Neurofilaments or microtubules correlated significantly with cross-sectional area at all axon levels (Fig. 9). The correlation was as strong as or stronger for the sum of these two organelles as for either organelle by itself; however, the slopes of correlation curves at levels before axon expansion were different from those after expansion (Fig. 9). When caliber expanded, a disproportionately small total number of microtubules and neurofilaments were needed to maintain the larger cross-sectional area at the 1,200-μm level (170 MT and NF/μm²) than at the (293 MT + NF/μm²) 50-μm level (Fig. 9). This observation raised the possibility that factors other than the absolute number of organelles contributed to the caliber expansion.

Carboxyl-Terminal Phosphorylation Is Associated with Increased Obligatory and Average Distance between Neurofilaments

Because carboxyl-terminal domains of NF-H and NF-M may serve as neurofilament side-arms, we investigated whether or not the additional contribution to caliber expansion might be a phosphorylation-induced increase in the minimum, or "obligatory", distance between neurofilaments. This possibility was clearly suggested by visual inspection of axons at levels proximal and distal to the caliber expansion (Fig. 10). The less phosphorylated neurofilaments at the 50-μm level appeared to cluster and be closer to their neighbors than the heavily phosphorylated neurofilaments present at 1,200 microns. These observations were confirmed by morphometric analyses on populations of 25 axons of comparable caliber distribution at each of the six axonal levels. For each neurofilament in these axons, the distance to its nearest neighbor was measured. The data on neurofilament distances for all axons were pooled at each level to reveal the percentage of neurofilaments exhibiting any particular spacing (Fig. 11). At the three most proximal axonal levels (0–100 μm), neurofilaments were spaced an average of 32.1 ± 11.1 nm from their nearest neighbor within a minimum spacing of 10–15 nm. The average interneurofilament distance was 1.7-fold higher (54.7 ± 17.9 nm) and the obligatory spacing increased to 20–25 nm at the 700- and 1,200-μm levels. It

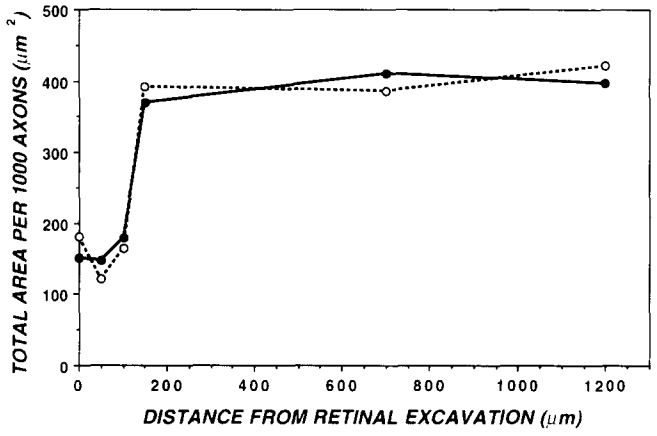

Figure 7. Changes in the calibers of axons at different levels of the proximal optic nerve. To facilitate comparisons across levels, the data for individual axons are pooled and the axonal cross-sectional area is expressed as total area per 1,000 axons. Each data point (*closed circles*) reflects caliber determinations of 2,500–3,000 axons. A separate population of 300–370 axons at each level used in the morphometric analyses of neurofilament and microtubule number (see Fig. 8) are shown (*open circles*) to demonstrate that the axons selected are an accurate representation of the actual caliber distribution at that level of the optic nerve.

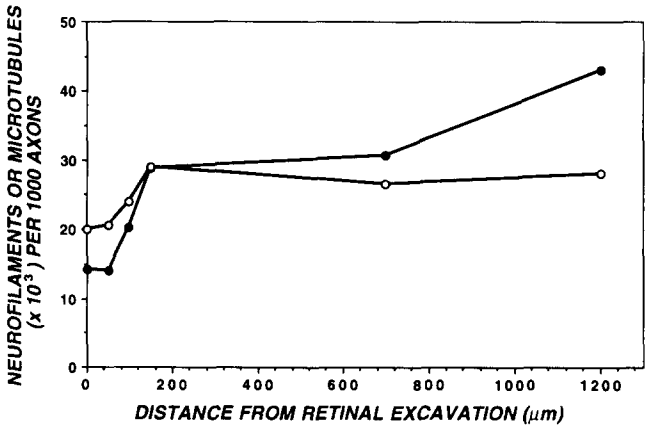

Figure 8. Changes in neurofilament and microtubule numbers at different levels along optic axons. Neurofilaments (*closed circles*) and microtubules (*open circles*) were counted manually in electron micrographs (80,000 ×) of transversely sectioned optic axons. From 300 to 370 axons were analyzed at each of the six levels. To facilitate comparisons across levels, data are expressed as number of neurofilaments or microtubules contained in 1,000 axons of sizes representative of the caliber distribution at that level.

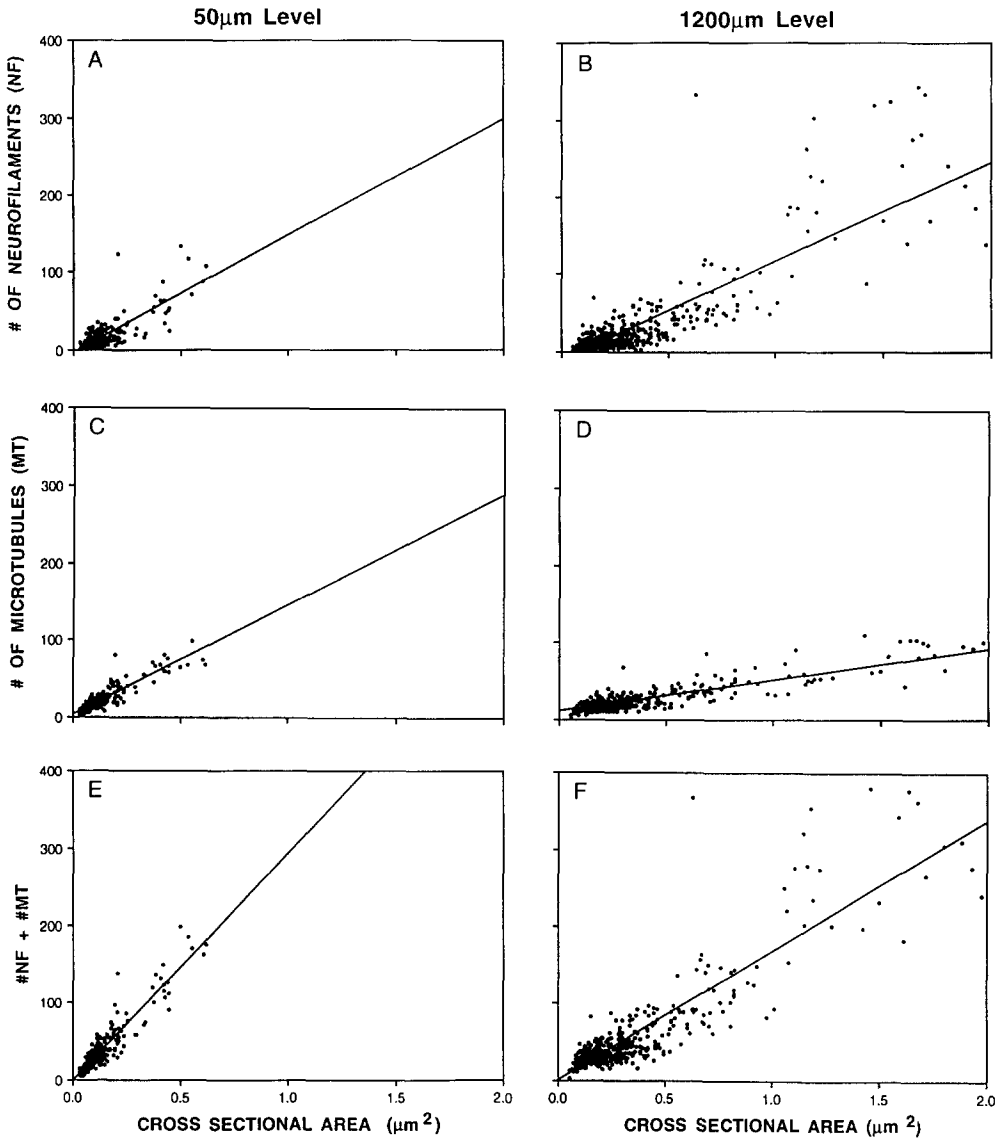

Figure 9. Relationship of neurofilaments and microtubules to axonal cross-sectional area at a representative level (50 μm) proximal to the site of extensive carboxyl-terminal phosphorylation, and a level (1,200 μm) distal to this site. The number of neurofilaments (*A* and *B*) or microtubules (*C* and *D*) or the sum of these structures (*E* and *F*) in each of 300–370 axons of representative size is plotted against the cross-sectional axoplasmic area in square microns. Correlation coefficients are 0.67, 0.70, 0.83, 0.80, 0.87, and 0.80 for *A–E*, respectively. After phosphorylation (at levels beyond 150 μm), a larger caliber size is maintained with proportionately fewer neurofilaments plus microtubules than at levels proximal to 150 μm.

is noteworthy that the majority of neurofilaments still displayed a characteristic spacing of 42 ± 10 nm. Neurofilaments at the 150-μm level exhibited obligatory and average spacing that were intermediate between the values at more proximal or distal levels. When the data for individual axons at each level were analyzed, the interneurofilament distances calculated for the pooled groups in Fig. 11 were evident, regardless of the caliber or neurofilament content of the axon (data not shown).

Myelination Influences Neurofilament Phosphorylation and Axon Caliber

The observation that myelin begins to appear at the same level of the optic nerve where caliber begins to expand (see Fig. 2) was further investigated in quantitative ultrastructural analyses of myelinated and unmyelinated fibers. These results confirmed that no axon profiles were myelinated proximal to the 150-μm level. Beginning at this level, however, the percentage of myelinated profiles in the total fiber population increased to more than 60% by 250 μm and 90–95% by the 1,200-μm level, beyond which the percentage was relatively constant (Fig. 12). Comparisons of myelinated and unmyelinated fiber populations at the 700-μm level demonstrated that only myelinated fibers displayed neurofilament accumulations and caliber expansion (Fig. 13, Table I). Similar results were seen at the 1,200-μm level (data not shown). Profiles that remained unmyelinated at the 700- and 1,200-μm levels had caliber distributions similar to those at proximal levels (0–100 μm from the eye) (Fig. 13). Moreover, the numbers of neurofilaments and microtubules that were in unmyelinated axons at the 700- and 1,200-μm levels were not increased relative to the numbers at more proximal axonal levels. In fact, neurofilaments were substantially less numerous in the unmyelinated fiber population at 700-μm and 1,200-μm than in the total population at the 0–100-μm levels (Table I), reflecting intrinsic differences in neurofilament content between axons that remain unmyelinated and axons that become myelinated more distally. Average nearest neighbor neurofilament distances and the distribution of these distances in unmyelinated axons containing

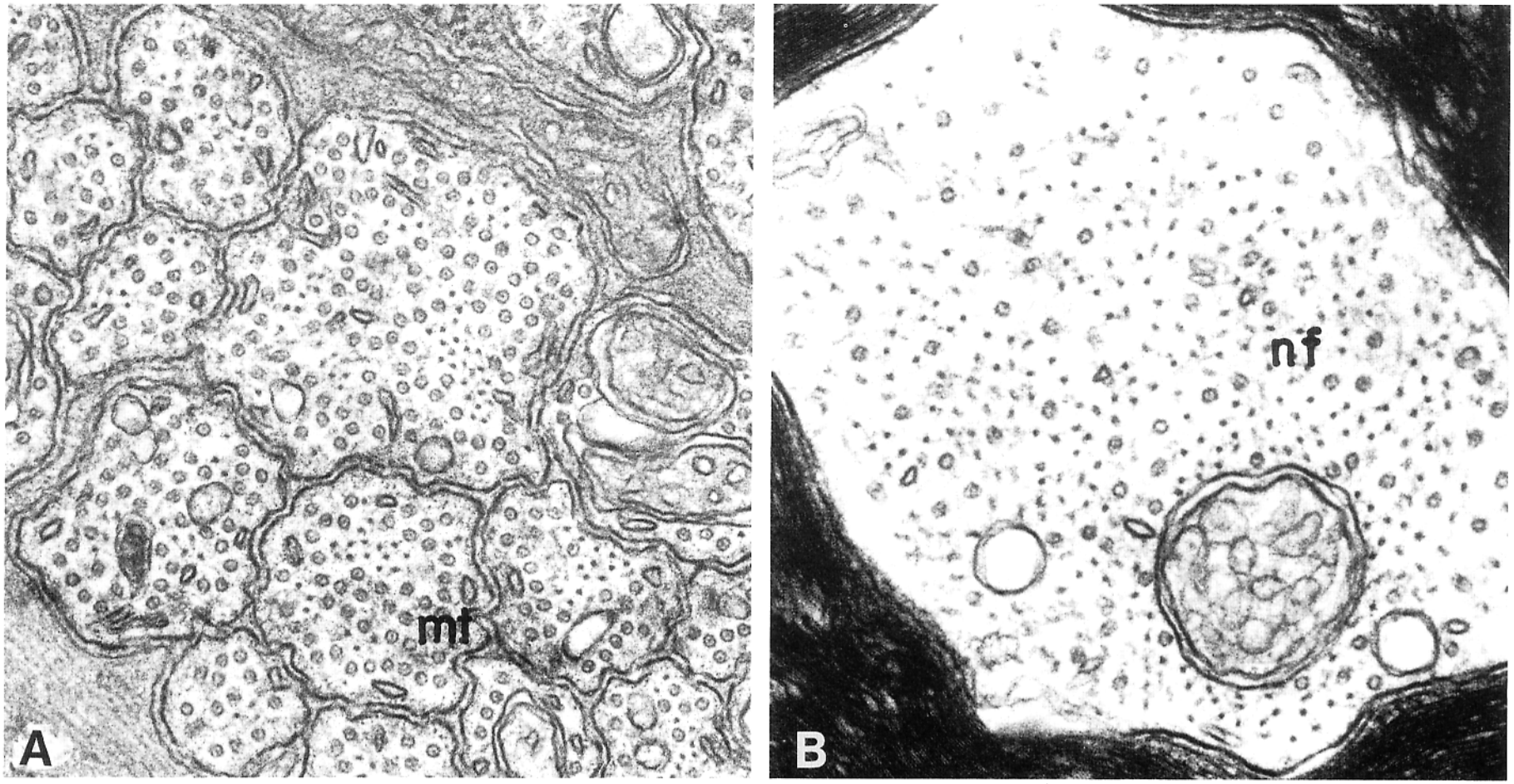

Figure 10. Ultrastructural appearance of ganglion cell axons at a level of the optic nerve proximal to the site of extensive carboxyl-terminal NF-H and NF-M phosphorylation (*A*, 50 μm from the retinal excavation) or distal to it (*B*, 700 μm from the excavation). Neurofilaments (*nf*) and microtubules (*mt*) are indicated on the micrographs.

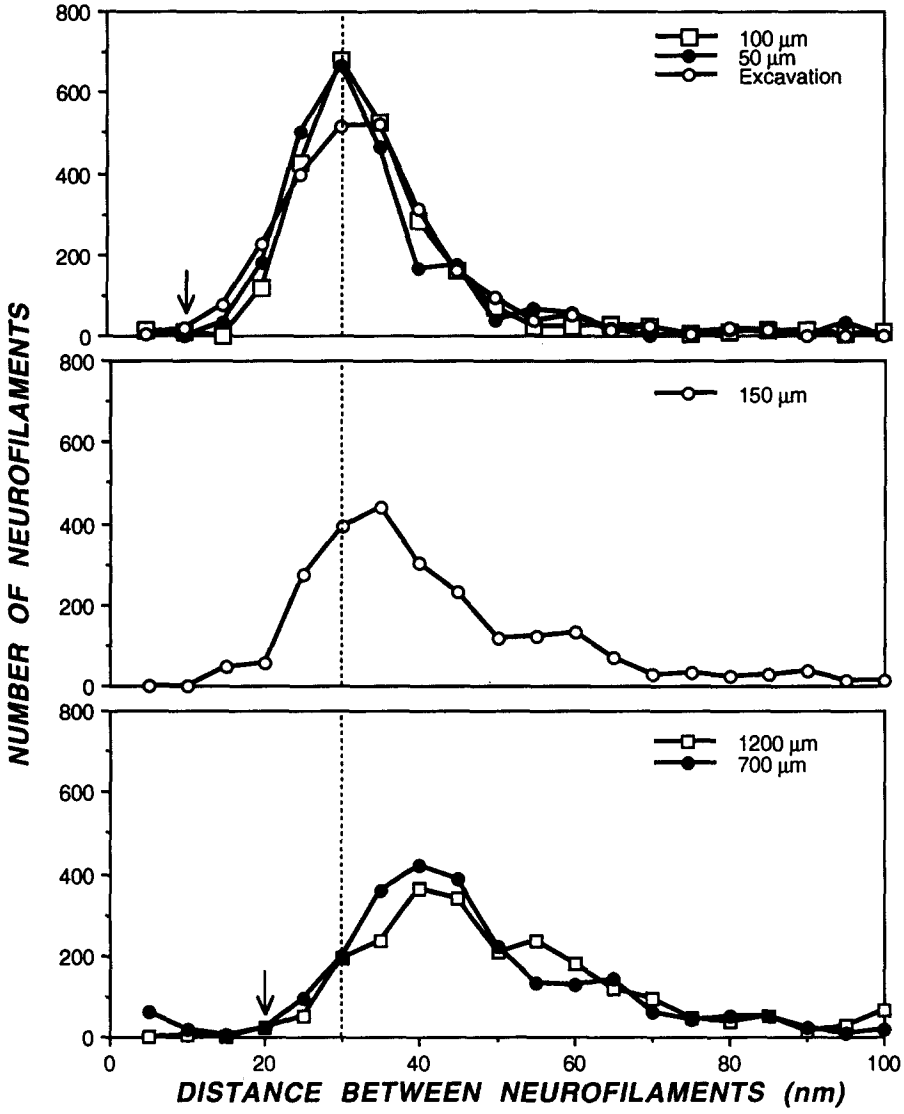

Figure 11. Nearest neighbor analysis of interneurofilament spacing. In populations of 25 axons at the indicated axonal level, the percentage of neurofilaments in the total population exhibiting nearest neighbor distances is given. For each neurofilament in an axon, the distance to its nearest neighboring neurofilament was measured as described in Materials and Methods. The shift in minimal neurofilament distance is indicated by the change in position of the two arrows.

more than five neurofilaments at the 700- and 1,200-μm levels did not significantly differ from those of myelinated axon profiles at the corresponding levels (Table I). As in myelinated axons, the majority of neurofilaments in unmyelinated axons displayed a characteristic spacing (48 ± 12 nm).

Discussion

The Site of Carboxyl-Terminal Domain NF-H Phosphorylation in Axons

By several different criteria, we have shown that the carboxyl-terminal domain of NF-H subunits in retinal ganglion cells begins to be heavily phosphorylated when transported neurofilaments reach a discrete proximal region of the axon within the optic nerve. Identification of the axon as the principal site of active carboxyl-terminal tail phosphorylation on transported neurofilaments accords with previous observations that axons but not perikarya are strongly immunostained by most antibodies against phosphorylation-dependent epitopes on the tails (Sternberger and Sternberger, 1983; (Drager et al., 1984; Lee et al., 1986; Trojanowski et al., 1986), NF-H and NF-M carboxyl-tail domain phosphorylation is delayed after subunit synthesis (Bennett and DiLullo, 1985; Oblinger et al., 1987; Glicksman et al., 1987; Nixon et al., 1990) and phosphate addition continues during neurofilament transport (Nixon et al., 1987, 1989*b*). We identified a distinct boundary 150–200 μm from the retinal excavation, which was defined by loss of SMI32 immunoreactivity and appearance of RT97 immunoreactivity. A similar sharp boundary has been observed in hamster optic nerve using SMI 32 antibody (Sloan and Stevenson, 1987). This transition between relatively hypophosphorylated NF-H subunits and extensively phosphorylated NF-H isoforms was unexpectedly sharp given the fact that the distances from individual ganglion cell bodies to this site in the optic nerve are heterogeneous. It is significant, however, that axons become ensheathed with myelin beginning at this level of the optic nerve and that extrinsic factors related to myelination have been shown to influence neurofilament phosphorylation (deWaegh et al., 1992). (Also see below.)

Phosphorylation of NF-H and NF-M tail domains within the multiphosphorylation repeat (MPR) region is believed to be a stepwise process (Lee et al., 1988; Clark and Lee,

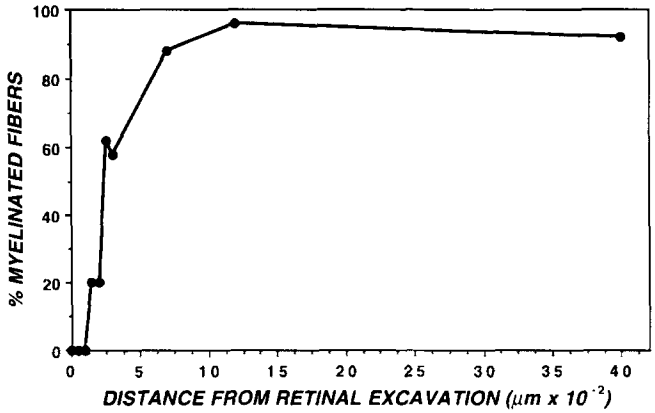

Figure 12. Relative proportions of myelinated axon profiles at different levels along the optic nerve. The numbers of unmyelinated and myelinated axons were determined from electron micrographs at 12,000 × magnification. Axon populations were the same as those analyzed in Fig. 7.

1991), which may begin in the perikaryon (Shea et al., 1990). Consistent with this idea is the observation that the monoclonal antibody SMI31, which recognizes initial stages of MPR phosphorylation (the P[+] phosphorylation state of Lee et al., 1988), began to decorate ganglion cell axons close to the perikaryon and recognizes a Triton-extractable pool of NF-H in the perikarya and initial segments (Shea et al., 1990). By contrast, RT97, an antibody recognizing the p(+++) state (Lee et al, 1988), began to decorate neurofilament proteins only at sites distal to the 150–200-μm active phosphorylation zone (Nixon et al., 1990). Other evidence also suggests that appearance of the RT97 epitope signals the attainment of a specific conformational state and reflects a high degree of phosphorylation of MPR and/or other carboxyl-terminal tail sites on NF-H (Coleman and Anderton, 1990; Clark and Lee, 1991; Roder and Ingram, 1991; Brion et al., 1993). Similarly, diminished immunostaining by SMI32, which recognizes MPR domains (particularly NF-H) only in their unphosphorylated state (Lee et al., 1988; Harris et al., 1991), also implies an increasing level of NF-H tail domain phosphorylation. This stage of phosphorylation occurs later after subunit synthesis than other phosphorylation events on the three subunits, including those on the amino-terminal head domain of NF-L and NF-M (Sihag and Nixon, 1991) and carboxyl terminus of NF-L (Nixon and Lewis, 1986; Sihag and Nixon, 1991). These findings indicate, therefore, that appearance of the most mature isoforms of NF-H and NF-M (Lewis and Nixon, 1988; Nixon et al., 1989*a*), reflecting a late stage of carboxyl-terminal phosphorylation, is what distinguishes neurofilaments beyond the 150-μm level of the optic nerve from those immediately proximal to this level.

Regulatory Influences of Carboxyl-Terminal Phosphorylation on Neurofilament Dynamics and Steady-State Levels

At the level where RT97 immunoreactivity appeared, neurofilaments began to accumulate markedly, a total of 3.0-fold within ~1 mm. Previous studies show further that phosphorylation of NF-H and NF-M tails continues along the

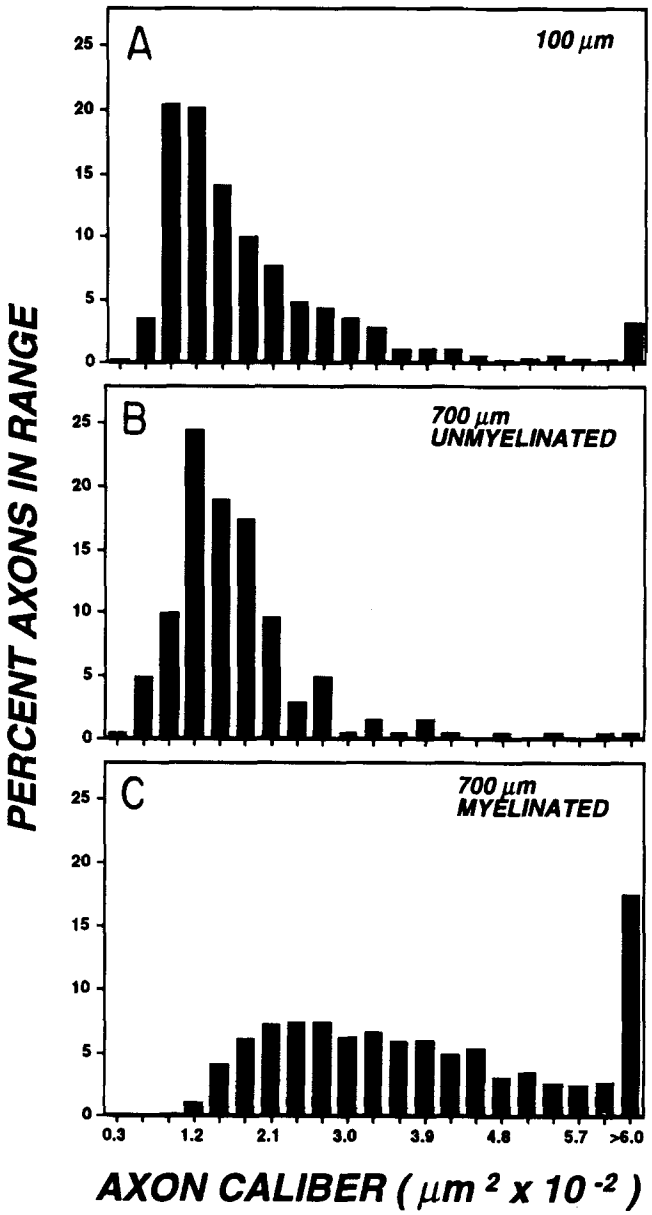

Figure 13. Axon caliber distributions for myelinated and unmyelinated fiber populations. The number of axons in each size class, expressed as a percentage of total axonal population analyzed, is plotted as a function of axon cross-sectional area. The total axon population (all unmyelinated, n = 1849) at the 100-μm level (*A*) is compared with the unmyelinated (n = 201) (*B*) and myelinated (n = 1462) (*C*) fibers present 700 μm from the retinal excavation.

entire length of optic axons (Nixon et al., 1987) and neurofilament number doubles again (Nixon and Logvinenko, 1986), resulting in a total sixfold increase in neurofilaments proximally to distally (0–7 mm from the eye). These increases in neurofilament number, and especially the initial doubling in neurofilaments over an axonal distance of only 50–100 μm, must reflect an abrupt and substantial change in the kinetics of neurofilament transport. The modest changes in microtubule number indicate that the changes in neurofilament dynamics are unique rather than a general effect on slow axonal transport mechanisms.

The marked non-uniform accumulation of neurofilaments

Table I. Regional Morphometrics of Myelinated and Unmyelinated Optic Axons

	Distance from retinal excavation				
	Unmyelinated profiles			Myelinated profiles	
	0 μm	700 μm	1,200 μm	700 μm	1,200 μm
Neurofilaments/1,000 axons	14,302	7,157	8,826	35,997	45,207
Microtubules/1,000 axons	20,082	15,114	15,043	29,086	28,855
Axons analyzed	539	70	23	313	358
Nearest neighbor distance (nm)*	32 ± 11	65 ± 13	58 ± 21	53 ± 18	55 ± 14
Axons analyzed	25	40	41	31	39

* Values are expressed as mean ± SD.

along ganglion cell axons implies that transport of some neurofilaments slows precipitiously or stops for considerable periods of time. Extensive phosphorylation of carboxyl tails in the region of the axon where neurofilaments double in number strongly supports the hypothesis that neurofilament transport is regulated in part by the phosphorylation of NF-H and NF-M (Lewis and Nixon, 1988; Watson et al., 1991; deWaegh et al., 1992). Previously we found that pulse-labeled neurofilaments retained along axons for long periods after the slow transport wave has passed contain mainly the most highly phosphorylated isoforms of NF-H (Lewis and Nixon, 1988) and NF-M (Nixon et al., 1989*a*). The data presented here show that these particular phosphovariants begin to be generated in axons precisely at the level where neurofilaments begin to accumulate. These results also accord with previous observations that the capacity of neurofilaments to interconnect in vitro into a reticulated network is lost when they become dephosphorylated (Eyer and Leterrier, 1988).

Regulation of Interneurofilament Spacing by Carboxyl-Terminal Phosphorylation

The extensive phosphorylation of the tail domains, particularly on a highly repeated motif, has led to speculations that increasing negative charge would rigidify and extend side-arms that maintain an obligatory distance between individual neurofilaments (Brown and Eagles, 1986; Carden et al., 1987), although in vitro studies of carboxyl-tail phosphorylation on isolated neurofilaments have been unsupportive (Hisanaga and Hirokawa, 1988). The present study of intact axons in vivo, however, provides strong evidence that phosphorylation events at carboxyl terminus domains of NF-H and NF-M substantially increase the minimum and average distance between neurofilaments. The length of the fully extended tail domains has been previously estimated by low-angle rotary shadowing to be 63 nm for NF-H and 55 nm for NF-M (Hisanaga and Hirokawa, 1988). The average distance of 25–35 nm that we measured between the neurofilaments at axonal levels 0–100 μm from the retinal excavation implies that these tail domains are either not fully elongated or are not fully perpendicular to the filament core. As NF-H and NF-M subunits attained a mature state of carboxyl-tail phosphorylation more distally along the axon, the average spacing between neurofilaments increased to 55 nm—a distance closer to that predicted for fully extended side-arms.

After carboxyl-terminal phosphorylation, neurofilaments were less closely spaced and clustered; however, their distribution in the radial dimension was not random. Interactions between neurofilaments were suggested from the fact that more than 50% of the neurofilaments exhibited the minimum obligatory spacing (45–65 nm) from their nearest neighbor, even in axons where the cross-sectional area could easily accommodate greater spacing.

The Role of Neurofilament Phosphorylation in Regulating Axon Caliber

In myelinated nerves, axon caliber is a principal determinant of conduction velocity (Hursh, 1939), a fundamental physiologic property of neurons. Observations that the caliber shifts during normal neuronal maturation (Hoffman et al., 1984; Hoffman et al., 1985*b*), axotomy (Hoffman et al., 1987; Oblinger and Lasek, 1988), and during axonal regeneration (Hoffman et al., 1985*b*; Hoffman and Cleveland, 1988) involve commensurate changes in neurofilament levels have supported the view that neurofilaments are a major determinant of axon caliber (Hoffman et al., 1984). Our results showing that neurofilaments accumulate regionally in relation to a local expansion of caliber along individual axons of normal mature mice further strengthens this hypothesis.

In developing or regenerating neurons, shifts in neurofilament levels accompanying caliber changes are mediated at least partly by changes in neurofilament mRNA (Julien et al., 1986; Lieberburg et al., 1989; Schlaepfer and Bruce, 1990) and protein synthesis (Lasek et al., 1983). Our findings suggest that, in addition to these factors, posttranslational mechanisms are critical to axonal caliber regulation. Carboxyl-terminal phosphorylation promoted caliber expansion in two different ways. First, by triggering the incorporation of some neurofilaments into a stationary network and possibly slowing the movement of others, phosphorylation prolonged the time neurofilaments reside in axons and thereby markedly increased their steady-state levels. This is advantageous because it would enable neurons to expand axon caliber with little or no increase in neurofilament gene expression. By eliminating the need for continuous replacement of the entire cytoskeleton at the rate of slow transport, neurons can maintain a large network of neurofilaments with fewer newly synthesized neurofilaments. The process also endows neurons with the ability to regulate neurofilament accumulation locally within the axon as observed here along optic axons, and in other systems at nodes of Ranvier (Reles and Friede, 1991; deWaegh et al., 1992; Mata et al., 1992) and at branch points or sharp turns along growing axons seeking their targets (Landmesser and Swain, 1992).

As a second mechanism to regulate caliber, carboxyl-terminal phosphorylation enhanced the space-occupying properties of the neurofilament network by increasing the minimum spacing between neurofilaments. A relationship between neurofilament density and carboxyl-terminal phosphorylation has also been recently reported (deWaegh et al., 1992; Mata et al., 1992). Arithmetic increases in interneurofilament spacing may exponentially increase space-filling capacity because the side-arms would be expected to create a spherical domain around the radial axis of the filament. This mechanism provides axons with considerable latitude for regulating axon caliber rapidly and reversibly without necessarily changing the number of neurofilaments. Both of these effects of carboxyl-terminal phosphorylation are relevant to observations that increasing the number of neurofilaments composed of only NF-L subunits does not necessarily cause caliber expansion (Monteiro et al., 1990) in transgenic mice overexpressing the NF-L gene. In the absence of the high molecular mass subunits, these neurofilaments would not be responsive to the posttranslational mechanisms that maximize their space-occupying capabilities.

The Influence of Myelination on Neurofilament Phosphorylation and Axon Caliber

Our results implicate myelination or events associated with myelination as a critical influence on the changes in neurofilament dynamics and axon caliber expansion. Myelin initially appeared on axons beginning at the 150-μm level of the optic nerve where caliber and neurofilament number abruptly increase. The subset of optic axons that remain unmyelinated along their entire length did not accumulate neurofilaments or undergo caliber expansion. Preliminary studies also indicate that the timing of the caliber expansion at the proximal axonal "transition" zone during postnatal development of the optic nerve coincides with the onset of myelin ensheathment (Nixon, R. A., P. A. Paskevich, I. Sanchez, L. Hassinger, unpublished observations). These results on normal central nervous system axons are in agreement with recent studies of peripheral fibers in the trembler myelin-deficient mutant mouse, showing an influence of myelinating Schwann cells on neurofilament phosphorylation and axon caliber (DeWaegh et al., 1992). Because astrocytes are commonly apposed to axons that are not myelinated, we cannot exclude the possibility that inhibitory influences of these cells are part of the signal that regulates these local axonal events (Geisert and Stewart, 1991; Baehr and Bunge, 1990).

Neurofilaments in unmyelinated fibers at 700- and 1,200-μm levels exhibited the same average nearest neighbor distances as those in myelinated fibers at these levels, suggesting that interneurofilament spacing and neurofilament accumulation are regulated independently by phosphorylation. If the neurofilament spacing observed at 0–100 μm is representative of all fiber types, which appears to be the case from Fig. 11, it indicates that neurofilament spacing in unmyelinated fibers increases distally as observed for myelinated fibers. This raises the possibility that myelination might influence certain events in adjacent unmyelinated axons. In any event, changes in interneurofilament distance in unmyelinated fibers would be expected to have little impact on caliber because, in these fibers, neurofilaments are few and the more numerous microtubules and membranous organelles are the major determinants of caliber size (Sasaki-Sherrington et al., 1984).

The astrocytic specialization located between 50–150 μm, known as the lamina cribrosa, could not explain the regional neurofilament and caliber differences along axons because unmyelinated optic axons maintained the same caliber and number of neurofilaments along regions either within the lamina cribrosa or distal to it. A modest effect of this structure in restricting fiber expansion, however, may be suggested by the observation that the densities of neurofilaments and microtubules were 30–40% higher within the region of the lamina cribrosa than at levels proximal or distal to it. The presence of a lamina cribrosa may, therefore, contribute slightly to the striking abruptness of the caliber expansion at 150 μm where this structure ends and myelination begins.

Implications for Axonal Transport Models

Regional accumulations of neurofilaments with or without a change in caliber can be explained if neurofilaments exist in multiple kinetic pools in axons (Nixon and Logvinenko, 1986; Nixon and Sihag, 1991). Variations on this concept have been proposed in which neurofilaments or neurofilament proteins drop off the axonal transport carrier for long periods and exchange with a stationary but dynamic cytoskeletal network within which moving neurofilaments may interact for brief or very long periods (Ochs et al., 1989; Hirokawa, 1991; Nixon and Sihag, 1991; Okabe et al., 1993; Okabe and Hirokawa, 1990, 1993). In confirmation of earlier observations (Nixon and Logvinenko, 1986), recent studies demonstrate that a pool of pulse-radiolabeled neurofilament proteins remains in axons for many months after slowly moving neurofilaments have exited (Nixon, R. A., K. B. Logvinenko, M. Mercken, S. Matthysse, and R. K. Sihag. 1993. Multiple cytoskeletal proteins contribute to a stationary but dynamic network in axons. *Soc. Neurosci. Abstr.* 19:61). These retained neurofilaments distribute non-uniformly along axons in a pattern identical to that of the entire axonal neurofilament pool, and their relative distribution does not change over at least 4 mo. Because of their exceptionally long half-life in axons, these neurofilaments, which we termed relatively stationary, are the major contributors to the total steady-state neurofilament pool in optic axons.

Non-uniform accumulation of neurofilaments along regions of both expanding and uniform caliber is not easily explained by a transport model in which the steady-state pool of neurofilaments is viewed as a single pool of continuously moving neurofilaments (Lasek et al., 1992). Generation of the sixfold proximal-to-distal differential in neurofilament number seen along the entire length of optic axons would require a commensurate slowing of the average neurofilament transport rate; however, movement of a pulse-labeled neurofilament wavefront along optic axon occurs at a relatively constant rate (Black and Lasek, 1980; Nixon and Logvinenko, 1986). In contrast to a single pool model, incorporation of a small proportion of transported neurofilaments into a slowly turned over stationary network could induce marked accumulation of neurofilaments without necessarily changing the rate of progression of the neurofilament wavefront. As a variation of a multiple kinetic pool concept, regional increases in steady-state neurofilament levels could

conceivably be generated by slowing of a subpopulation of the total neurofilament pool; however, at least half of the moving pulse-labeled neurofilaments exit the optic tract at roughly the same rate that they enter axons and another 20–30% move 2–3-fold more slowly (Nixon and Logvinenko, 1986) (Nixon, R. A., K. B. Logvinenko, M. Mercken, S. Matthysse, and R. K. Sihag. 1993. Multiple cytoskeletal proteins contribute to a stationary but dynamic network in axons. *Soc. Neurosci. Abstr.* 19:61). (Lasek et al., 1992). Net movement of the remaining fraction of neurofilaments would, consequently, have to be exceedingly slow to generate the observed sixfold increment in steady-state neurofilament levels along optic axons. The kinetics of this pool would, therefore, be qualitatively distinct from the other moving neurofilaments and have essentially the same characteristics as neurofilaments that we have termed stationary (Nixon and Logvinenko, 1986) to emphasize that they are not moving during most of their long residence time in axons.

We thank Drs. Itzhak Fischer, Marc Mercken, Ivelisse Sánchez, and Thomas Shea for valuable discussion and comments on the manuscript. We are grateful to Dr. Thomas Shea for providing neurofilament antibodies, Timothy Wheelock for assistance with cryostat sectioning, Linda Hassinger for technical assistance, Kate Nixon for artwork, and Johanne Khan for typing and assistance with manuscript preparation.

This research was supported by a grant from the National Institute on Aging (AG05604).

Received for publication 21 January 1994 and in revised form 25 May 1994.

References

Anderton, B. H., D. Breinburg, M. J. Downes, P. J. Green, B. E. Tomlinson, J. Ulrich, J. W. Wood, and J. Kahn. 1982. Monoclonal antibodies show that neurofibrillary tangles and neurofilaments share antigenic determinants. *Nature (Lond.).* 298:84–86.

Baehr, M., and R. P. Bunge. 1990. Growth of adult rat retinal ganglion cell neurites on astrocytes. *Glia.* 3:293–300.

Bennett, G. S., and C. DiLullo. 1985. Slow postranslational modification of a neurofilament protein. *J. Cell Biol.* 100:1799–1804.

Black, M. M., and R. J. Lasek. 1980. Slow components of axonal transport: two cytoskeletal networks. *J. Cell Biol.* 86:616–623.

Brion, J.-P., A.-M. Couck, J. Robertson, T. L. F. Loviny, and B. H. Anderton. 1993. Neurofilament monoclonal antibodies RT97 and 8D8 recognize different modified epitopes in paired helical filament-τ in Alzheimer's disease. *J. Neurochem.* 60:1372–1382.

Brown, A., and P. A. Eagles. 1986. Squid neurofilaments. Phosphorylation and Ca^{2+}-dependent proteolysis *in situ*. *Biochem. J.* 239:191–197.

Carden, M. J., W. W. Schlaepfer, and V. M.-Y. Lee. 1985. The structure, biochemical properties, and immunogenicity of neurofilament peripheral regions are determined by phosphorylation state. *J. Biol. Chem.* 260:9805–9817.

Carden, M. J., J. Q. Trojanowski, W. W. Schlaepfer, and V. M.-Y. Lee. 1987. Two-stage expression of neurofilament polypeptides during rat neurogenesis with early establishment of adult phosphorylation patterns. *J. Neurosci.* 7:3489–3504.

Chiu, F.-C., and W. T. Norton. 1982. Bulk preparation of CNS cytoskeleton and the separation of individual neurofilament proteins by gel filtration: dye-binding characteristics and amino acid compositions. *J. Neurochem.* 39:1252–1260.

Clark, E. A., and V. M.-Y. Lee. 1991. Dynamics of mammalian high-molecular-weight neurofilament subunit phosphorylation in cultured rat sympathetic neurons. *J. Neurosci. Res.* 30:116–123.

Coleman, M. P., and B. H. Anderton. 1990. Phosphate dependent monoclonal antibodies to neurofilaments and Alzheimer neurofibrillary tangles recognize a synthetic phosphopeptide. *J. Neurochem.* 54:1548–1555.

Dahl, D. 1981. Isolation of neurofilament proteins and of immunologically active neurofilament degradation products from extracts of brain, spinal cord and sciatic nerve. *Biochem. Biophys. Acta.* 668:229–306.

Dahl, D., and A. Bignami. 1986. Neurofilament phosphorylation in development: a sign of axonal maturation? *Exp. Cell Res.* 162:220–230.

Dahl, D., C. J. Crosby, E. E. Gardner, and A. Bignami. 1986. Delayed phosphorylation of the largest neurofilament protein in rat optic nerve development. *J. Neurosci. Res.* 15:513–519.

Dahl, D., M. Grossi, and A. Bignami. 1984. Masking of epitopes in tissue sections. A study of glial fibrillary acidic (GFA) protein with antisera and monoclonal antibodies. *Histochemistry.* 81:525–531.

DeWaegh, S. M., V. M.-Y. Lee, and S. T. Brady. 1992. Local modulation of neurofilament phosphorylation, axonal caliber, and slow axonal transport by myelinating Schwann cells. *Cell.* 68:451–463.

Dräger, U. C., and J. F. Olsen. 1981. Ganglion cell distribution in the retina of the mouse. *Invest. Ophthalmol. Vis. Sci.* 20:285–293.

Dräger, U. C., D. L. Edwards, and C. J. Barnstable. 1984. Antibodies against filamentous components in discrete cell types of the mouse retina. *J. Neurosci.* 4:2025–2042.

Eyer, J., and J.-F. Leterrier. 1988. Influence of the phosphorylation state of neurofilament proteins on the interactions between purified filaments *in vitro*. *Biochem. J.* 252:655–660.

Foster, G. A., D. Dahl, and V. M.-Y. Lee. 1987. Temporal and topographic relationships between the phosphorylated and nonphosphorylated epitopes of the 200 kDa neurofilament protein during development *in vitro*. *J. Neurosci.* 7:2651–2663.

Franke, W. W. 1987. Nuclear lamins and cytoskeletal intermediate filament proteins: a growing multigene family. *Cell.* 48:3–4.

Geisert, E. E., Jr., and A. M. Stewart. 1991. Changing interactions between astrocytes and neurons during CNS maturation. *Dev. Biol.* 143:335–345.

Geisler, N., E. Kaufmann, S. Fischer, U. Plessman, and K. Weber. 1983. Neurofilament architecture combines structural principles of intermediate filaments with carboxyl-terminal extensions increasing in size between triplet proteins. *EMBO (Eur. Mol. Biol. Organ.) J.* 2:1295–1302.

Geisler, N., J. Vandekerckhove, and K. Weber. 1987. Location and sequence characterization of the major phosphorylation sites of the high molecular mass neurofilament proteins M and H. *FEBS (Fed. Eur. Biochem. Soc.) Lett.* 221:403–407.

Gill, S. R., P. C. Wong, M. J. Monteiro, and D. W. Cleveland. 1990. Assembly properties of dominant and recessive notations in the small mouse neurofilament (NF-L) subunit. *J. Cell Biol.* 111:2005–2019.

Glicksman, M. A., D. Soppet, and M. B. Willard. 1987. Posttranslational modifications of neurofilament polypeptides in rabbit retina. *J. Neurobiol.* 18:167–196.

Goldstein, M. E., L. A. Sternberger, and N. H. Sternberger. 1987. Varying degrees of phosphorylation determine microheterogeneity of the heavy neurofilament polypeptide (NF-H). *J. Neuroimmunol.* 14:135–148.

Harris, J., C. Ayyub, and G. Shaw. 1991. A molecular dissection of the carboxyterminal tails of the major neurofilament subunits NF-M and NF-H. *J. Neurosci. Res.* 30:47–62.

Hirokawa, N. 1991. Molecular architecture and dynamics of the neuronal cytoskeleton. *In* The Neuronal Cytoskeleton. R. D. Burgoyne, editor. J. Wiley & Sons, New York. 5–74.

Hirokawa, N., M. A. Glicksman, and M. Willard. 1984. Organization of mammalian neurofilament polypeptides within the neuronal cytoskeleton. *J. Cell Biol.* 98:1523–1536.

Hisanaga, S., and N. Hirokawa. 1988. Structure of the peripheral domains of neurofilaments revealed by low angle rotary shadowing. *J. Mol. Biol.* 202:297–305.

Hisanaga, S., Y. Gonda, M. Inagaki, A. Ikai, and N. Hirokawa. 1990. Effects of phosphorylation of the neurofilament L protein on filamentous structures. *Cell Reg.* 1:237–248.

Hoffman, P.N., and R. J. Lasek. 1975. The slow component of axonal transport: identification of major structural polypeptides of the axon and their generality among mammalian neurons. *J. Cell Biol.* 66:351–366.

Hoffman, P. N., and D. W. Cleveland. 1988. Neurofilament and tubulin expression recapitulates the developmental program during axonal regeneration: induction of a specific β-tubulin isotype. *Proc. Natl. Acad. Sci. USA.* 85:4530–4533.

Hoffman, P. N., D. W. Cleveland, J. W. Griffin, P. W. Landes, N. J. Cowan, and D. L. Price. 1987. Neurofilament gene expression: a major determinant of axonal caliber. *Proc. Natl. Acad. Sci. USA.* 84:3472–3476.

Hoffman, P. N., J. W. Griffin, B. G. Gold, and D. L. Price. 1985*a*. Slowing of neurofilament transport and the radial growth of developing nerve fibers. *J. Neurosci.* 5:2920–2929.

Hoffman, P. N., G. W. Thompson, J. W. Griffin, and D. L. Price. 1985*b*. Changes in neurofilament transport coincide temporally with alterations in the caliber of axons in regenerating motor fibers. *J. Cell Biol.* 101: 1332–1340.

Hoffman, P. N., J. W. Griffin, and D. L. Price. 1984. Control of axonal caliber by neurofilament transport. *J. Cell Biol.* 99:705–714.

Hsu, S.-M., L. Raine, and H. Fanger. 1981. Use of avidin-biotin-peroxidase complex (ABC) in immunoperoxidase techniques: a comparison between ABC and unlabeled antibody (PAP) procedures. *J. Histochem. Cytochem.* 29:577–580.

Hursh, J. B. 1939. Conduction velocity and diameter of nerve fibers. *Am. J. Physiol.* 127:131–139.

Julien, J.-P., and W. E. Mushynski. 1983. The distribution of phosphorylation sites among identified proteolytic fragments of mammalian neurofilaments. *J. Biol. Chem.* 258:4019–4025.

Julien, J.-P., D. Meijer, J. Hurst, and F. Grosveld. 1986. Cloning and developmental expression of the murine neurofilament gene family. *Mol. Brain Res.*

1:243–250.
Kaufmann, E., N. Geisler, and K. Weber. 1984. SDS-PAGE strongly overestimates the molecular masses of the neurofilament proteins. *FEBS (Fed. Eur. Biochem. Soc.) Lett.* 170:81–88.
Laemmli, U. K. 1970. Cleavage of structural proteins during the assembly of the head of bacteriophage T4. *Nature (Lond.).* 227:680–685.
Landmesser, L., and S. Swain. 1992. Temporal and spatial modulation of a cytoskeletal antigen during peripheral axonal pathfinding. *Neuron.* 8:291–305.
Lasek, R. J., M. M. Oblinger, and P. F. Drake. 1983. The molecular biology of neuronal geometry: the expression of neurofilament genes influences axonal diameter. *Cold Spring Harbor Symp. Quant. Biol.* 48:731–744.
Lasek, R. J., P. Paggi, and M. J. Katz. 1992. Slow axonal transport mechanisms move neurofilaments relentlessly in mouse optic axons. *J. Cell Biol.* 117:607–616.
Lazarides, E. 1982. Intermediate filaments: a chemically heterogeneous, developmentally regulated class of proteins. *Annu. Rev. Biochem.* 51:219–250.
Lee, V. M.-Y., M. J. Carden, and J. Q. Trojanowski. 1986. Novel monoclonal antibodies provide evidence for the *in situ* existence of a nonphosphorylated form of the largest neurofilament subunit. *J. Neurosci.* 6:850–858.
Lee, V. M.-Y., M. J. Carden, W. W. Schlaepfer, and J. Q. Trojanowski. 1987. Monoclonal antibodies distinguish several differentially phosphorylated states of the two largest rat neurofilament subunits (NF-H and NF-M) and demonstrate their existence in the normal nervous system of adult rats. *J. Neurosci.* 7:3474–3488.
Lee, V. M.-Y., L. Otvos, Jr., M. J. Carden, M. Hollosi, B. Dietzschold, and R. A. Lazzarini. 1988. Identification of the major multiphosphorylation site in mammalian neurofilaments. *Proc. Natl. Acad. Sci. USA.* 85:1998–2002.
Lees, J. F., P. S. Schneidman, S. F. Skuntz, J. J. Carden, and R. Lazzarini. 1988. The structure and organization of the heavy neurofilament subunit (NF-H). *EMBO (Eur. Mol. Biol. Organ.) J.* 7:1947–1955.
Leterrier, J. F., R. K. H. Liem, and M. L. Shelanski. 1982. Interactions between neurofilaments and microtubule associated proteins: a possible mechanism for intraorganellar bridging. *J. Cell Biol.* 95:982–986.
Lewis, S. E., and R. A. Nixon. 1988. Multiple phosphorylated variants of the high molecular mass subunit of neurofilaments in axons of retinal cell neurons: characterization and evidence for their differential association with stationary and moving neurofilaments. *J. Cell Biol.* 107:2689–2701.
Lieberburg, I., N. Spinner, S. Snyder, J. Anderson, D. Goldgaber, M. Smulowitz, Z. Carroll, B. Emanuel, J. Breitner, and L. Rubin. 1989. Cloning of a cDNA encoding the rat high molecular weight neurofilament peptide (NF-H): developmental and tissue expression in the rat, and mapping of its human homologue to chromosomes 1 and 11. *Proc. Natl. Acad. Sci. USA.* 86:2463–2467.
Liem, R., and S. Hutchinson. 1982. Purification of the neurofilament triplet: filament assembly from the 70,000 dalton subunit. *Biochemistry.* 21: 3221–3226.
Liem, R. K. H., S.-H. Yen, G. D. Salomon, and M. L. Shelanski. 1978. Intermediate filaments in nervous tissue. *J. Cell Biol.* 79:637–645.
Mack, K., J. R. Currie, and D. Soifer. 1988. cDNA coding for the tail region of the high molecular weight rabbit neurofilament protein NF-H. *J. Neurosci. Res.* 20:129–136.
Marotta, C. A., P. Strocchi, and J. M. Gilbert. 1979. Biosynthesis of heterogeneous forms of mammalian brain tubulin subunits by multiple messenger RNAs. *J. Neurochem.* 33:231–246.
Mata, M., M. Kupina, and D. J. Fink. 1992. Phosphorylation-dependent neurofilament epitopes are reduced at the node of Ranvier. *J. Neurocytol.* 21: 199–210.
Monteiro, M. J., P. N. Hoffman, J. D. Gearhart, and D. W. Cleveland. 1990. Expression of NF-L in both neuronal and nonneuronal cells of transgenic mice: increased neurofilament density in axons without affecting caliber. *J. Cell Biol.* 111:1543–1557.
Nakamura, Y., M. Takeda, K. J. Angelides, T. Tanaka, K. Tada, and T. Nishimura. 1990. Effect of phosphorylation on 68 kDa neurofilament subunit protein assembly by the cyclic AMP dependent protein kinase *in vitro*. *Biochem. Biophys. Res. Commun.* 169:744–750.
Nixon, R. A. 1980. Protein degradation in the mouse visual system I. Degradation of axonally transported and retinal proteins. *Brain Res.* 200:69–83.
Nixon, R. A. 1992. Slow axonal transport. *Curr. Opin. Cell Biol.* 4:8–14.
Nixon, R. A. 1993. The regulation of neurofilament protein dynamics by phosphorylation: clues to neurofibrillary pathobiology. *Brain Pathol.* 3:29–38.
Nixon, R. A., and S. E. Lewis.1986. Differential turnover of phosphate groups on neurofilament subunits in mammalian neurons *in vivo*. *J. Biol. Chem.* 261:16298–16301.
Nixon, R. A., and K. B. Logvinenko. 1986. Multiple fates of newly synthesized neurofilament proteins: evidence for a stationary neurofilament network distributed nonuniformly along axons of retinal ganglion cell neurons. *J. Cell Biol.* 102:647–659.
Nixon, R. A., and R. K. Sihag. 1991. Neurofilament phosphorylation: a new look at regulation and function. *Trends Neurosci.* 14(11):501–506.
Nixon, R. A., B. A. Brown, and C. A. Marotta. 1982. Posttranslational modification of a neurofilament protein during axoplasmic transport: implications for regional specialization of CNS axons. *J. Cell Biol.* 94:150–158.
Nixon, R. A., I. Fischer, and S. E. Lewis. 1990. Synthesis, axonal transport, and turnover of the high molecular weight microtubule-associated protein MAP 1A in mouse retinal ganglion cells: tubulin and MAP 1A display distinct transport kinetics. *J. Cell Biol.* 110:437–448.
Nixon, R. A., S. E. Lewis, and C. A. Marotta. 1987. Posttranslational modification of neurofilament proteins by phosphate during axoplasmic transport in retinal ganglion cell neurons. *J. Neurosci.* 7:1145–1158.
Nixon, R. A., S. E. Lewis, and R. K. Sihag. 1989*a*. One of multiple phosphorylated variants of the middle neurofilament subunit (NF-M) preferentially associates with neurofilaments in the stationary axonal cytoskeleton. *J. Neurochem.* 52(Suppl.):561.
Nixon, R. A., S. E. Lewis, D. Dahl, C. A. Marotta, and U. C. Dräger. 1989*b*. Early posttranslational modifications of the three neurofilament subunits in mouse retinal ganglion cells: neuronal sites and time course in relation to subunit polymerization and axonal transport. *Mol. Brain Res.* 5:93–108.
Oblinger, M. M., and R. J. Lasek. 1988. Axotomy-induced alterations in the synthesis and transport of neurofilament and microtubules in dorsal root ganglion cells. *J. Neurosci.* 8:1747–1758.
Oblinger, M. M., S. T. Brady, I. G. McQuarrie, and R. J. Lasek. 1987. Cytotypic differences in the protein composition of the axonally transported cytoskeleton in mammalian neurons. *J. Neurosci.* 7:453–462.
Ochs, S., R. A. Jersild, and J. M. Li. 1989. Slow transport of freely movable cytoskeletal components shown by beading partition of nerve fibers in the cat. *Neuroscience.* 33:421–430.
Okabe, S., and N. Hirokawa. 1990. Turnover of fluorescently labelled tubulin and actin in the axon. *Nature (Lond.).* 343:479–482.
Okabe, S., and N. Hirokawa. 1993. Do photobleached fluorescent microtubules move? Re-evaluation of fluorescence laser photobleaching both in vitro and in growing Xenopus axon. *J. Cell Biol.* 120:1177–1186.
Okabe, S, H. Miyasaka, and N. Hirokawa. 1993. Dynamics of the neuronal intermediate filaments. *J. Cell Biol.* 121:375–386.
Pant, H. D., G. Shecket, H. Gainer, and R. J. Lasek. 1978. Neurofilament protein is phosphorylated in the squid giant axon. *J. Cell Biol.* 78:R23–R27.
Radius, R. L. 1981. Regional specificity in anatomy at the lamina cribrosa. *Arch. Ophthalmol.* 99:478–480.
Reles, A., and R. L. Friede. 1991. Axonal cytoskeleton at the nodes of Ranvier. *J. Neurocytol.* 20:450–458.
Roder, H. M., and V. M. Ingram. 1991. Two novel kinases phosphorylate tau and the KSP site of heavy neurofilament subunits in high stoichiometric ratios. *J. Neurosci.* 11:3325–3343.
Sasaki-Sherrington, S. E., J. R. Jacobs, and J. K. Stevens. 1984. Intracellular control of axial shape in non-uniform neurites: a serial electron microscopic analysis of organelles and microtubules in AI and AII retinal amacrine neurites. *J. Cell Biol.* 98:1279–1290.
Schlaepfer, W. W., and J. Bruce. 1990. Simultaneous up-regulation of neurofilament proteins during the postnatal development of the rat nervous system. *J. Neurosci. Res.* 25:39–49.
Sharpe, G. A., G. Shaw, and K. Weber. 1982. Immuno-electron microscopical localization of the three neurofilament proteins along neurofilaments in a cultured dorsal root ganglion cells. *Exp. Cell Res.* 137:403–413.
Shaw, G. 1991. Neurofilaments in the neuronal cytoskeleton. R. D. Burgoyne, editor. J. Wiley & Sons, New York. 5–74.
Shaw, G., and K. Weber. 1982. Differential expression of neurofilament triplet proteins in brain development. *Nature (Lond.).* 298:276–299.
Shea, T. B., R. K. Sihag, and R. A. Nixon. 1990. Dynamics of phosphorylation and assembly of the high molecular weight neurofilament subunit in NB2a/dl neuroblastoma. *J. Neurochem.* 55:1784–1792.
Sihag, R. K., and R. A. Nixon. 1989. *In vivo* phosphorylation of distinct domains of the 70-kilodalton neurofilament subunit involves different protein kinases. *J. Biol. Chem.* 264:457–464.
Sihag, R. K., and R. A. Nixon. 1990. Phosphorylation of the amino-terminal head domain of the middle molecular mass 145 kDa subunit of neurofilaments: evidence for regulation by second messenger-dependent protein kinases. *J. Biol. Chem.* 265:4166–4171.
Sihag, R. K., and R. A. Nixon. 1991. Identification of Ser-55 as a major protein kinase A phosphorylation site on the 70-kDa subunit of neurofilaments: early turnover during axonal transport. *J. Biol. Chem.* 266:18861–18867.
Skalli, O., and R. D. Goldman. 1991. Recent insights into the assembly, dynamics, and function of intermediate filament networks. *Cell Motil. Cytoskeleton.* 19:67–79.
Sloan, K. E., and J. A. Stevenson. 1987. Differential distribution of phosphorylated and non-phosphorylated neurofilaments within the retina and optic nerve of hamsters. *Brain Res.* 437:365–368.
Steinert, P. M., and D. R. Roop. 1988. Molecular and cellular biology of intermediate filaments. *Annu. Rev. Biochem.* 57:593–625.
Sternberger, L. A., and N. H. Sternberger. 1983. Monoclonal antibodies distinguish phosphorylated and nonphosphorylated forms of neurofilaments *in situ*. *Proc. Natl. Acad. Sci. USA.* 80:6126–6130.
Sternberger, N. H., L. A. Sternberger, and J. Ulrich. 1985. Aberrant neurofilament phosphorylation in Alzheimer disease. *Proc. Natl. Acad. Sci. USA.* 82:4274–4276.
Takeuchi, K. S., K.-I. Saito, and R. A. Nixon. 1992. Immunoassay and activity of calcium-activated neutral proteinase (mCANP): distribution in soluble and membrane-associated fractions in human and mouse brain. *J. Neurochem.* 58:1526–1532.
Trojanowski, J. Q., N. Walkenstein, and V. M.-Y. Lee. 1986. Expression of neurofilament subunits in neurons of the central and peripheral nervous sys-

tem: an immunohistochemical study with monoclonal antibodies. *J. Neurosci.* 6:650–660.

Watson, D. F., P. N. Hoffman, and J. W. Griffin. 1991. Phosphorylation-related immunoreactivity and the rate of transport of neurofilaments in chronic 2,5-hexanedione intoxication. *Brain Res.* 539:103–109.

Willard, M., and C. Simon. 1981. Antibody decoration of neurofilaments. *J. Cell Biol.* 89:198–205.

Willard, M., and C. Simon. 1983. Modulations of neurofilament axonal transport during the development of rabbit retinal ganglion cells. *Cell.* 36: 551–559.